Enhanced In-vivo Optical Imaging of the Inflammatory Response to Acute Liver Injury in C57Bl/6 Mice using a Highly Bright Near-Infrared BODIPY Dye

Dumitru Sirbu,[a] Saimir Luli,[b] Jack Leslie,[b] Fiona Oakley,[b] and Andrew C. Benniston*[a]

Abstract: Delving deeper is possible in whole body *in vivo* imaging using a super-bright membrane targeting BODIPY dye (**BD**). The dye was employed to monitor homing of *ex vivo*, fluorescently labelled neutrophils to an injured liver of dark pigmented C57BL/6 mice. *In Vivo* Imaging System (IVIS) data conclusively showed an enhanced signal intensity and a higher signal-to-noise ratio in mice receiving neutrophils labelled with the **BD** dye compared to those labelled with a gold standard dye at 2 hr post *in vivo* administration of fluorescently labelled cells. Fluorescence-activated cell sorting (FACS) confirmed that **BD** was non-toxic, and an exceptional cell labelling dye that opens up precision deep organ *in vivo* imaging of inflammation in mice routinely used for biomedical research. The origin of enhanced performance is identified with the molecular structure, and the distinct localisation of the dye within cells that enable remarkable changes in its optical parameters.

Chronic liver disease is prevalent in many developed countries and the incidence of disease is rising year-on-year due to viral infection, alcohol consumption and the obesity epidemic.[1] In response to liver damage, immune cells are recruited to the site of injury and initiate wound repair. In chronic disease, inflammation and scar cells persist, causing fibrosis and eventually organ failure.[2] More generally, inflammation is a key driver of chronic disease, cancer and is a feature of ageing.[3] Whilst we validate use of the **BD** dye to monitor damage-induced hepatic inflammation, this methodology is readily transferable and can be exploited to monitor inflammation in any organ during acute or chronic disease. Developing techniques that help illuminate inflammatory processes will ultimately advance our understanding of disease pathology and provide tools to assess treatment response.[4] An emerging technology is focused on optical recording using an *In Vivo* Imaging System (IVIS)[5] combined with direct labelling of cells with a lipophilic fluorescent dye; it is frequently used to longitudinally track cells to study disease biology[6] and test new drugs within a whole animal.[7] The applications of IVIS include: (i) the monitoring inflammation and recruitment of immune cells to a site of injury,[8] (ii) visualization of immune cell:tumour interactions[9] and (iii) the assessment of the biodistribution and migration of cell-based therapies.[10]

Whole body minimally-invasive imaging provides spatial and temporal information that can provide a better understanding of cell behavior,[11] or monitor a therapeutic response in the native environment.[12] Moreover, high-resolution molecular imaging of fluorescent labelled cells in vivo is also feasible through optical windows surgically implanted into the skin of mice to view an organ with fluorescence microscopes.[13] A limitation of fluorescence-based IVIS imaging is that many employed fluorescent dyes are often not tailor-made for a specific purpose, fluoresce within the autofluorescence range (*ca.,* 450-560 nm), are not sufficiently bright to penetrate tissue, rapidly photobleach, have broad excitation and emission spectra which restricts multiplex imaging capabilities or are cytotoxic.[14] The cyanine dye CellVue Burgundy 710 **CD** (Figure 1) is generally recognized as a gold standard lipophilic dye for cell membrane labelling, and is frequently used in conjunction with IVIS for *in vivo* cell tracking.[15]

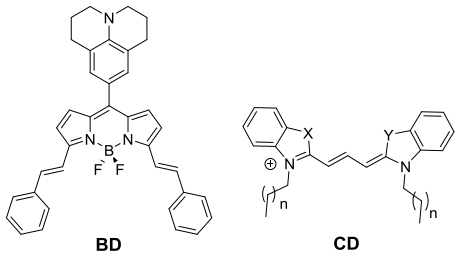

Figure 1. Chemical structure of the NIR fluorescent derivative **BD** used in IVIS along with the core structure of the common dye CellVue Burgundy 710 (**CD**) used for cell tracking. Note: X and Y are heteroatoms to tune the photophysical properties of the dye.

Although **CD** is used in *in vivo* cell monitoring its application is often limited to nude or albino mice and/or in disease models where pathology is superficially localized (i.e., skin).[16] Nude and albino mice do not develop skin pigmentation and provide a level of tissue transparency, leading to enhanced photon penetrance. C57Bl/6 mice are the preferred strain for preclinical mouse models because the majority of transgenic mice are generated on this background, and unlike nude mice, which lack T-cells, C57Bl/6 mice have a normal immune system. In medical research it is essential to study disease in orthotopic mouse models. The liver is a deep-seated organ and tissue depth provides a major barrier in signal detection. To overcome this technical challenge it is important to develop fluorophores that emit in the near infrared range (> 700 nm) and are compatible with other fluorescent imaging technologies (*e.g.,* FACS), which allow validation of *in vivo* data at the cellular level. In our line of research into producing optically responsive neuron firing probes the

[a] Prof A. C. Benniston and Dr D. Sirbu
Molecular Photonics Laboratory
Chemistry-School of Natural & Environmental Sciences
Newcastle University, Newcastle upon Tyne, NE1 7RU
E-mail:andrew.benniston@ncl.ac.uk
[b] Prof F. Oakley, Dr S. Luli, Dr J. Leslie
Newcastle Fibrosis Research Group, Institution of Cellular Medicine
Newcastle University, Newcastle upon Tyne, NE1 7RU

neutral Bodipy derivative **BD** (Figure 1) was developed.[17] As part of these studies it was noted that **BD** localized strongly in membranes with intense fluorescence in the near-infrared region.[18] Perceiving the potential for **BD** to track inflammatory cells using an IVIS to monitor acute liver damage, the dye was directly compared with the **CD** under identical conditions; **BD** outperforms **CD** in brightness and importantly, does not cause cell apoptosis. The basic dye structure also lends itself more easily to fine-tuning of emission characteristics, and secondary group attachment (*e.g.,* antibodies) via the aryl groups.

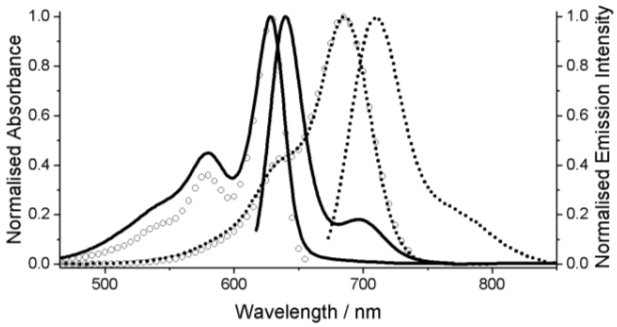

Figure 2. Room-temperature normalised UV/Vis-NIR absorption and emission spectra for compounds **BD** (solid line) and **CD** (dotted line) in cyclohexane. Excitation spectra are shown with open circles.

Absorption and fluorescence spectra for **BD** are shown in Figure 2. The long-wavelength absorption profile consists of a strong and narrow absorption band at 623 nm with a large broader appearance as a higher energy tail. To the low-energy side it can be noticed that the band does not exactly follow the Gaussian shape, and there is a tail stretching into the far-red region. This observation can be understood by looking at the frontier molecular orbitals (Figure 3). While HOMO and LUMO are mostly localized on the extended BODIPY core, the HOMO-1 is located preferentially on the julolidine unit. Thus, the lowest energy transition can be attributed to the BODIPY π-π* transition and the HOMO-1 to LUMO transition can be crudely described as a julolidine-BODIPY charge transfer transition. A TD-DFT calculation in cyclohexane predicts the energy of the two transitions to be 2.12 eV and 2.14 eV, respectively, so essentially a significant overlap of the two bands is expected (see Supporting Information). Deconvolution of the absorption profile into a series of Gaussians requires the use of three typical BODIPY bands and an additional broader band (Supporting Information). The two transitions are close in energy 624 nm and 566 nm respectively, in agreement with the TD-DFT results. The emission profile shows a band at 630 nm with a small Stokes shift, and is not the exact mirror image of the absorption spectrum due to the missing broad charge-transfer band. The excitation profile mostly mirrors the absorption spectrum except for the lower intensity of the high-energy shoulder, in line with the presence of a non-emissive excited state. The quantum yield of fluorescence (Φ_{FLU}) in cyclohexane is 0.75 with a fluorescence lifetime (τ_S) of 4.3 ns (Supporting Information). Fluorescence is partially quenched as the solvent polarity is increased because of stabilization of the charge transfer state, leading to a new non-radiative excited state decay pathway. The Φ_{FLU} for **BD** and **CD** in the membrane-like solvent oleic acid are 0.64 and 0.43, respectively. Given the higher molar absorption coefficient of **BD** (40,000 M^{-1} cm^{-1}) with respect to **CD** (22,000 M^{-1} cm^{-1}), one might expect its brightness to be *ca.* 2.7 times greater.[19]

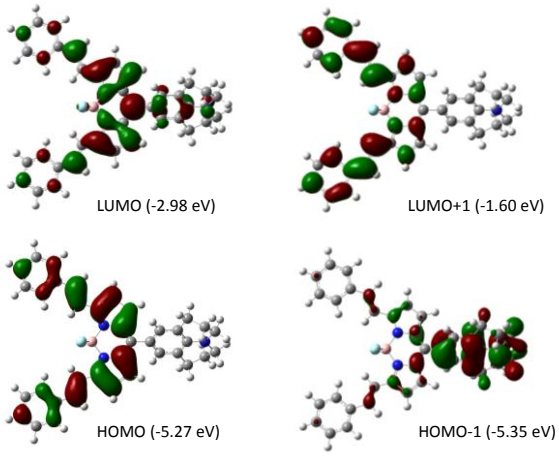

Figure 3. Representation of the Gaussian calculated Kohn–Sham frontier molecular orbitals for **BD** in cyclohexane using an IEF-PCM model at mPW1PW91/6-311+G(d,p) theoretical level.[20]

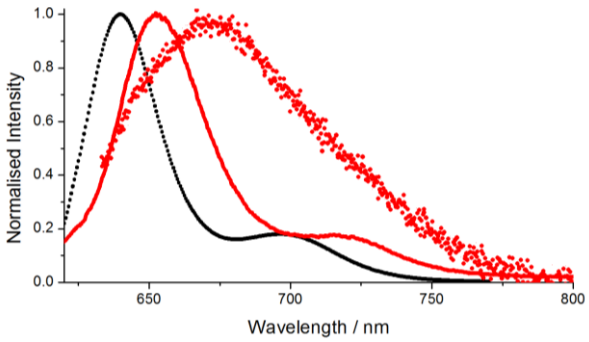

Figure 4. Room-temperature emission spectra for **BD** in oleic acid (black dotted line), 15 mM Triton X-100 solution in water (red solid line) and neutrophils cells in PBS buffer (red dots).

The emission profile of neutrophil cells in PBS stained with **BD** is dominated by a band at 670 nm, red-shifted and broadened as compared with the solution spectrum in oleic acid with relatively similar physical parameters compared to a cell membrane (Figure 4). This observation cannot be explained by stabilization of the excited state in an environment of a higher polarity as there are only marginal changes to the emission maxima when measured in the highly polar DMSO solvent. The broadening and redshift to 653 nm is repeated for the emission from micelles of Triton X-100 in water. This is indicative of selective positioning of the dye at the lipid-water interface that leads to a non-uniform solvation environment around the molecule, affecting the bandgap energy and hence to emission profile broadening. The redshift is attributed to a better stabilization of the excited state by the dual nature of the bilayer. From the point of view of fluorescence microscopy this shifts the signal of interest into the optical window of biological tissue. Emission from the dye exterior to cells is preferentially absorbed by tissue material, making **BD** a prime candidate for cells labelling and bioimaging purposes.[21]

To prove the potential of **BD** for the bioimaging of neutrophils, an immune cell subtype was labelled with **BD** and **CD** using an identical protocol already widely accepted in IVIS experiments.[22] Wild type C57BL/6 mice were administered a single intraperitoneal dose of carbon tetrachloride (CCl_4) to cause liver injury. 24 h post liver damage, recipient mice were injected intravenously with 10 million labelled neutrophils. The majority of

the neutrophils home to the liver in this model and are known to generally locate adjacent to the areas of injury surrounding the central vein regions and are distributed homogeneously across the different liver lobes. 2 h post cell administration whole body *in vivo* IVIS was used to monitor recruitment of fluorescently labelled neutrophils to the injured liver of mice. *In vivo* fluorescent signal was quantified by drawing region of interest (ROI) in the area where the liver is localised. Figure 5 shows the IVIS images of mice injected with **CD** or **BD** labelled neutrophils. The fluorescent overlay is observed in the upper quadrant of the abdominal area where the liver is situated. Compared to **CD**, **BD** labelled neutrophils provide significantly higher radiant efficiency, suggesting that **BD** is brighter and more readily detectable by IVIS. Although IVIS allows whole body imaging, signal to noise ratio is limited by tissue depth, but this study found that **BD** provided enhanced signal detection and photon penetration depth. **BD** can facilitate *in vivo* imaging of various biological processes in deep-seated organs without the need to sacrifice the animals.

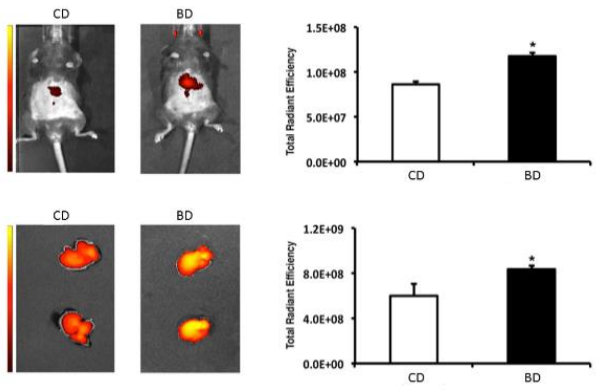

Figure 5. IVIS imaging of neutrophils labelled with **CD** or **BD**, tracking to the liver of mice with acute liver injury. IVIS images of mice (top) and ex vivo imaged livers (bottom) and graph showing the fluorescence signal as total radiant efficiency. Total radiant efficiency is mean ± s.e.m, n = 4 recipient mice/ group. Statistical significance was determined using an unpaired t-test, *P < 0.05.

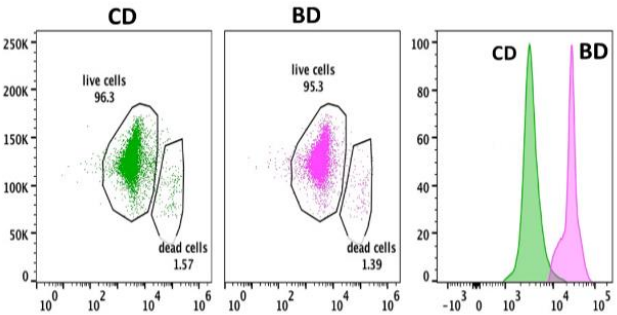

Figure 6. FACS plots showing comparison of ex vivo labelled murine neutrophils with **CD** and **BD**. (live/dead cells are circled). Right FACS plot showing the comparative brightness in log scale of **BD** compared to **CD**.

To validate that the *in vivo* signal originated from the liver, mice were humanely killed, and the liver excised and then *ex vivo* imaged on the IVIS (Figure 5). A similar bright fluorescence signal was observed for the *ex vivo* images, the signal detection was significantly higher in the liver of mice injected with **BD** labelled neutrophils compared to those labelled with **CD**. Our data shows that **BD** is far superior to **CD** for the application of non-invasive, whole body fluorescence cell-tracking. The enriched intense fluorescence of **BD** offers a clear advantage of detecting a reduced number of cells, thus increasing the sensitivity of the technique in detecting smaller areas of interest. **BD** provides an ideal tool to monitor cell infiltration in deep-seated organs of wild type mice, as it overcomes the main challenges associated with *in vivo* optical imaging, such as tissue depth and black skin pigmentation. This methodology is not limited to studying damage-induced hepatic inflammation, but can be adapted to various orthotopic mouse models. A significant advantage of **BD** is that it can be applied to various genetic mouse models generated on the C57bl/6 background.

Fluorescence-activated cell sorting (FACS) methodology was used to separate the fluorescently labelled neutrophils recruited to the injured liver, based on their spectral signature compared to other unlabeled liver cells. A very low cytotoxicity was found for both dyes, with only 1.6 % dead cells for **CD** and a marginal improvement of 1.4 % for **BD** (Figure 6). Furthermore, FACS was also applied to assess fluorescent signal intensity. A log plot of comparative brightness proves **BD** provides an order of magnitude more intense emission signal (Figure 6). This supports once again the superiority of the dye in labeling neutrophil cells for imaging purposes.

In conclusion, the unique properties of **BD** have been used to open new possibilities for the *in vivo* imaging technique.[23] The unusually strong red-shift of the emission from the neutrophils allowed for significantly brighter signals in all the attempted experiments, and more importantly during the whole body IVIS imaging of CCl_4 injured liver of mice with **BD** labelled neutrophils. The enhanced signal-to-noise ratio and low cytotoxicity allows performing the previously inaccessible fine-imaging experiments on live specimens. The dye also allows imaging of fewer cells, currently a limiting factor for IVIS cell tracking, because of the lower detection limit possible in terms of the numbers of cells that can be identified. Given the enhanced brightness and narrow excitation profile of **BD** we are currently investigating its use in concomitantly identifying more than one cell type by multiplex spectral imaging.

Experimental Section

All chemicals were purchased from commercial sources and used as received unless otherwise stated. Solvents for spectroscopic investigations were of the highest purity available. The title compound **BD** was available from previous studies[17] and purified by column chromatography before use and its purity checked by NMR spectroscopy. Quantum yields of fluorescence were measured by the comparison method using AzaBODIPY (5,5-difluoro-3,7-bis(4-methoxyphenyl)-1,9-5H-4λ4,5λ4−dipyrrolo[1,2-c:2',1-f[1,3,5,2]triazaborinine).[24] Selected data are shown in Table S1.

Computational calculations were performed using a 32-bit version of Gaussian09 on a quadruple-core Intel Xeon system with 4GB RAM. The calculations were run in parallel, fully utilising the multi-core processor. Firstly, the structure of **BD** was optimised with the DFT mPW1PW91/3-21G method and the result was used as the input for calculations at the mPW1PW91/6-311+G(d,p) without any symmetry constraint in cyclohexane solvent using an IEF-PCM model. Energy minimization calculations were monitored using the programme Molden and run in parallel with frequency calculations to ensure optimized geometries represented local minima. The electronic transitions of **BD** were calculated using IEF-PCM solvent model at mPW1PW91/6-311+G(d,p) theory level.

Electronic absorption spectra were recorded at RT using a Shimadzu UV-1800 spectrophotometer. Fluorescence emission spectra were acquired at RT with a Shimadzu RF-6000 fluorimeter. Fluorescence lifetimes were collected using a PTI EasyLife apparatus. Spectra deconvolution was performed using PeakFit software. IVIS experiements were carried out using a Perkin Elmer IVIS Spectrum *in-vivo* imaging system and neutrophils were imaged using a BD LSRFortessa™ X-20 (BD Biosciences) system. Data analysis was achieved using flowjo V10 software.

All experiments on mice were performed under approval from the Newcastle Ethical Review Committee and a UK Home Office licence. Prior to *in-vivo* fluorescence imaging neutrophils were labelled with either the BODIPY-based dye (**BD**) or the commercially available CellVue Burgundy 710 dye (**CD**) according to manufacture instructions. The concentration of the dye stock solution = 1mM in ethanol and the final neutrophil labelling concentration = 2 µM. The labelling time = 4 minutes.

Following successful cell labelling, CCl_4 injured mice were intravenously (IV) injected with 10 million fluorescently labelled neutrophils. 2 h post IV injection mice were anaesthetised under isoflurane and IVIS imaged using an excitation filter of 675 nm and an emission filter of 720 nm. After the final *in-vivo* scan mice were sacrificed and the livers were harvested for *ex-vivo* imaging using the same filter set as above.

The average radiant efficiency [p/s/cm^2/sr]/[µW/cm^2] for both *in-vivo* and *ex-vivo* images was analysed using Living Image 4.4 software. *In-vivo* scans were analysed by drawing regions of interest (ROI) in the upper quadrant of the abdomen, below the sternum to the middle of the abdominal region, where the liver is anatomically situated. *Ex-vivo* fluorescent signal was quantified by drawing triangular ROIs to encapsulate the liver.

Fluorescence confocal imaging was performed using murine neutrophils labelled with **BD** dye and fixed in 4% PFA in PBS for 20 minutes and then counterstained with DAPI. Confocal fluorescent images were taken using a Zeiss AxioImager upright microscope using Cy5 and DAPI filters.

Acknowledgements

We thank the Engineering & Physical Sciences Council (EPSRC) for the award of an Impact Accelerator Account (IAA) grant.

Keywords: *In-vivo* imaging • Liver • Fluorescence • Bodipy • Cell Sorting

[1] a) C. Baeck, A. Wehr, K. R. Karlmark, F. Heymann, M. Vucur, N. Gassler, S. Huss, S. Klussmann, D. Eulberg, T. Luedde, C. Trautwein, F. Tacke, *Hepatology*, **2012**, *61*, 416-426. b) T. Hardy, F. Oakley, Q. M. Anstee, C. P. Day, *Annu. Rev. Pathol. Mech. Dis.* **2016**, *11*, 451-96. c) M. Mantovania, G. Zazab, C. D. Byrne, A. Lonardoe, G. Zoppini, E. Bonoraa, G. Targhera, *Metabolism*, **2017**, *79*, 64-76.

[2] Y. A. Lee, M. C. Wallace, S. L. Friedman, *Gut*, **2015**, *64*, 830-841.

[3] S. A. Emming, T. A. Wynn, P. Martin, *Science*, **2017**, *356*, 1026-1030.

[4] a) B. D. Tarlow, M. J. Finegold, M. Grompe, *Hepatology*, **2014**, *60*, 278-289. (b) S. J. Forbes, P. N. Newsome, *Nat. Rev.,* **2016**, *13*, 473-485.

[5] a) H. Yukawa, Y. Baba, *Anal. Sci.* **2018**, *34*, 525-532. b) W. Zarychta-Wiśniewska, A. Burdzinska, R. Zagozdzon, B. Dybowski, M. Butrym, Z. Gajewski, L. Paczek, *PLoS ONE*, **2017**, *12*, e0184588. c) H. M. Park, K. A. Russo, G. Karateev, M. Park, E. Dubikovskaya, L. J. Kriegsfeld, A. Stahl, *Gastroenterology*, **2017**, *152* , 78-81. d) X. He, L. Li, Y. Fang, W. Shi, X. Lia, H. Ma, *Chem. Sci*. **2017**, *8*, 3479-3483.

[6] G. Follain, L. Mercier, N. Osmani, S. Harlepp, J. G. Goetz, *J. Cell. Sci*., **2017**, *130*, 23-38.

[7] S. Luli, D. Di Paolo, P. Perri, C. Brignole, S. J. Hill, H. Brown, J. Leslie, H. L. Marshall, M. C. Wright, D. A. Mann, M. Ponzoni, F. Oakley, *J. Hepatogy*, **2016**, *65*, 75-83.

[8] C. L. Wilson, D. Jurk, N. Fullard, P. Banks, A. Page, S. Luli, S., A. M. Elsharkawy, R. G. Gieling, J. B. Chakraborty, C. Fox, C. Richardson, K. Callaghan, G. E. Blair, N. Fox, A. Lagnado, J. F. Passos, A. J. Moore, G. R. Smith, J. Mann, F. Oakley, D. A. Mann, *Nat. Commun.,* **2015**, *6*, 6818.

[9] J. R. W. Conway, S. C. Warren, P. Timpson, *Methods*, **2017**, *128*, 78-94.

[10] S. P. Arlauckas, C. S. Garris, R. H. Kohler, M. Kitaoka, M. F. Cuccarese, K. S. Yang, M. A. Miller, J. C. Carlson, G. J. Freeman, R. M. Anthony, R. Weissleder, M. J. Pittet, *Sci. Transl. Med.,* **2017**, *9*, eaal3604.

[11] D. Lodygin, A. Flügel, *Cell Calcium*, **2017**, *64*, 118-129.

[12] Z. Gaoa, J. Suna, M. Gaob, F. Yua, L. Chena, Q. Chena, *Sensor Actuat. B-Chem*., **2018**, *265*, 565-574.

[13] a) J. Kim, D.-H. Kim, S. J. Jung, H.-J. Gil, S. Z. Yoon, Y.-I. Kim, K. S. Soh, *Biomed. Opt. Express*, 2016, *7*, 1251-1259. b) J. Gao, X. Peng, P. LI, Z. Ding, J. Qu, H. Niu, *Front. Optoelectron.*, **2015**, *8*, 170-176.

[14] J. Icha, M. Weber, J. C. Waters, C. Norden, *Bioessays*, **2017**, *39*, 1700003.

[15] The dye is a registered trademark of ThermoFisher Scientific and sold in a kit as a far-red/near-infrared fluorescent cell labelling reagent. The identity of X and n is unknown, but for cyanine dyes X is generally CMe_2, O, S or Se.

[16] M. Hassan, B. A. Klaunberg, *Comp. Med.*, 2004. *54*, 635-644.

[17] D. Sirbu, J. B. Butcher, P. G. Waddell, P. Andras, A. C. Benniston, *Chem-Eur. J.*, **2017**, *23*, 14639-14649.

[18] The calculated logP for the dye is 2.87 suggesting it is lipophilic and would be membrane targeting. The value is slightly less than for **CD** where X = O and n = 2 (logP = 3.36); the logP value increases with n and

where X = S. The superior fluorescence imaging for **BD** is probably not just a lipophilicity driven membrane targeting factor.

[19] Brightness is defined as (ε_{max} x ϕ_{FLU})/1000 and is often used to compare different dyes, by taking into account their dissimilar quantum yield and molar absorption coefficient. The equation clearly does not take into account selective uptake into a membrane or degradation effects that are important in the imaging of organs *in vivo*.

[20] Using the suite of packages in Gaussian 09: Frisch, M. J.; Trucks, G. W.; Schlegel, H. B.; Scuseria, G. E.; Robb, M. A.; Cheeseman, J. R.; Scalmani, G.; Barone, V.; Mennucci, B.; Petersson, G. A.; Nakatsuji, H.; Caricato, M.; Li, X.; Hratchian, H. P.; Izmaylov, A. F.; Bloino, J.; Zheng, G.; Sonnenberg, J. L.; Hada, M.; Ehara, M.; Toyota, K.; Fukuda, R.; Hasegawa, J.; Ishida, M.; Nakajima, T.; Honda, Y.; Kitao, O.; Nakai, H.; Vreven, T.; Montgomery, J. A., Jr.; Peralta, J. E.; Ogliaro, F.; Bearpark, M.; Heyd, J. J.; Brothers, E.; Kudin, K. N.; Staroverov, V. N.; Kobayashi, R.; Normand, J.; Raghavachari, K.; Rendell, A.; Burant, J. C.; Iyengar, S. S.; Tomasi, J.; Cossi, M.; Rega, N.; Millam, J. M.; Klene, M.; Knox, J. E.; Cross, J. B.; Bakken, V.; Adamo, C.; Jaramillo, J.; Gomperts, R.; Stratmann, R. E.; Yazyev, O.; Austin, A. J.; Cammi, R.; Pomelli, C.; Ochterski, J. W.; Martin, R. L.; Morokuma, K.; Zakrzewski, V. G.; Voth, G. A.; Salvador, P.; Dannenberg, J. J.; Dapprich, S.; Daniels, A. D.; Farkas, Ö.; Foresman, J. B.; Ortiz, J. V.; Cioslowski, J.; Fox, D. J. Gaussian, Inc., Wallingford CT, 2009.

[21] Confocal imaging confirmed that the **BD** dye efficiently labels the cell membrane of murine neutrophils (see Supporting Information for a typical image).

[21] Y. Yin, Y. Kwon, D. Kim, G. Kim, Y. Hu, J.-H. Ryu, J. Yoon, *Nat. Protocols*, **2015**, *10*, 1742-1754.

[22] For some examples of BODIPY-based imaging probes see: a) J.-S. Lee, N. Kang, Y. K. Kim, A. Samanta, S. Feng, H. K. Kim, M. Vendrell, J. H. Park, *J. Am. Chem. Soc.,* **2009**, *131*, 10077-10082. b) X. Liu, M. Wu, Q. Hu, H. Bai, S. Zhang, Y. Shen, *ACS Nano*, **2016**, *10*, 11385-11396. c) T. Kowada, J. Kikuta, A. Kubo, M. Ishii, H. Maeda, S. Mizukami, *J. Am. Chem. Soc*., **2011**, *133*, 17772-17776. d) T. Kowada, H. Maeda, k. Kikuchi, *Chem. Soc. Rev.,* **2015**, 44, 4953-4972. e) S. Koleman, E. U. Akkaya, *Coord. Chem. Rev.,* **2018**, 354, 121-134.

[23] J. K. G. Karlson, A. Harriman, A., *J. Phys. Chem. A,* **2016**, *120*, 2537-2546.

Blinded by the Light. A super-bright membrane targeting BODIPY dye opens up deep-seated organ imaging in full immune system mice.

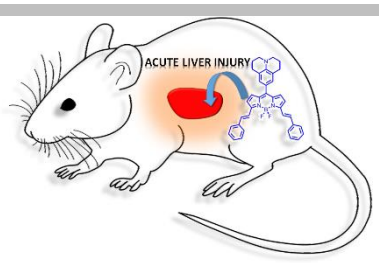

*Dumitru Sirbu, Saimir Luli, Jack Leslie, Fiona Oakley, Andrew C. Benniston**

Enhanced In-vivo Optical Imaging of the Inflammatory Response to Acute Liver Injury in C57Bl/6 Mice using a Highly Bright Near-Infrared BODIPY Dye